Beyond blooms: A novel time series analysis framework predicts seasonal keystone species and sheds light on ecosystem stability in the Fram strait

Ellen Oldenburg [1,2,3,◇,*], **Raphael M. Kronberg** [3,4,◇], **Katja Metfies** [5,6], **Wilken-Jon von Appen** [7], **Matthias Wietz** [3,8,9], **Christina Bienhold** [3,8], **Ovidiu Popa** [1,△] and **Oliver Ebenhöh** [1,2,△]

[1] *Institute of Theoretical and Quantitative Biology, Heinrich Heine University, Düsseldorf, 40225, North Rhine-Westphalia, Germany*

[2] *Cluster of Excellence on Plant Sciences, Heinrich Heine University, Düsseldorf, 40225, North Rhine-Westphalia, Germany*

[3] *Deep-Sea Ecology and Technology, Alfred Wegener Institute Helmholtz Centre for Polar and Marine Research, Bremerhaven, Germany*

[4] *Mathematical Modelling of Biological Systems, Heinrich Heine University, Düsseldorf, 40225, North Rhine-Westphalia, Germany*

[5] *Polar Biological Oceanography, Alfred-Wegener-Institut Helmholtz Center for Polar and Marine Research*

[6] *Helmholtz Institute for Functional Marine Biodiversity at the University of Oldenburg, Oldenburg, Germany*

[7] *Physical Oceanography of the Polar Seas, Alfred Wegener Institute Helmholtz Centre for Polar and Marine Research, Bremerhaven, Germany*

[8] *Max Planck Institute for Marine Microbiology, Bremen, Germany*

[9] *Institute for Chemistry and Biology of the Marine Environment,University of Oldenburg, Oldenburg, Germany*

Correspondence*:
Ellen Oldenburg - Universitätstraße 1, 40225 Düsseldorf, Germany
Ellen.Oldenburg@hhu.de

◇ Equal contribution and first authorship: These authors contributed equally to this work and share first authorship.
△ Last authorship: These authors share last authorship.

ABSTRACT

A thorough understanding of ecosystem functioning in the Arctic Ocean, a region under severe threat by climate change, requires detailed studies on inhabiting biological communities. The identification of keystone species with special ecological relevance is of great importance, yet difficult to achieve with established community assessments. In the case of microbes, metabarcoding and metagenomics offer fundamental insights into community structure and function, yet remain limited regarding conclusions about the role of individual species within the ecosystem. To overcome this limitation, we have developed an analytical approach based on three different methods: Co-Occurrence Networks, Convergent Cross Mapping, and Energy Landscape Analysis. These methods enable the identification of seasonal communities in microbial ecosystems, elucidate their interactions, and predict potential stable community configurations under varying environmental conditions. Combining the outcomes of these three methods allowed us to define 19 keystone species that are representative for the different trophic modes that build the local food web. They may serve as indicator species for monitoring the consequences of environmental change in Arctic marine ecosystems. Our research reveals a clear seasonal pattern in the composition of the microbial phytoplankton community, with distinct assemblages characterizing the carbon fixation (light) and consumption (dark) phases. Species interactions exhibit strong seasonality, and we observed summer communities with significant influence on winter communities but not vice versa. During spring thaw, two distinct groups are present: consumers (heterotrophs), strongly linked to the dark phase, and photoautotrophs (mainly Bacillariophyta), initiating growth (photoautotrophic Bacillariophyta). These groups are not causally related, suggesting a ”winter reset” with selective effects that facilitates a new blooming period, allowing survivors of the dark phase to emerge. Investigating the fragility of these ecological systems using Energy Landscape Analysis we demonstrate that winter communities are more stable than summer communities. In summary, the ecological landscape of the Fram Strait can be categorized by two distinct phases: a production phase governed by specialized organisms that are highly responsive to environmental changes, and a consumption phase dominated by generalist species with enhanced resilience.

Keywords: Cross Convergence Mapping, Co-Occurrence Network, Energy Landscape Analysis, Keystone species, Eukaryotes

1 INTRODUCTION

The Arctic Ocean and climate change

The Arctic Ocean is a unique ecosystem, that is currently undergoing a major transition due to the ongoing repercussions of climate change. Over the past two decades, Arctic surface temperatures have risen at a rate more than twice the global average (Meredith et al., 2019). This temperature amplification is linked to feedback mechanisms triggered by reductions in sea ice and snow cover, which exacerbate warming trends. In particular, the Arctic sea ice extent has been declining throughout the year, with the most pronounced decline occurring in September (Meredith et al., 2019). These environmental changes have a wide range of consequences, including profound shifts in biodiversity (Sala et al., 2000), and thus have a fundamental impact on ecosystems of the Arctic Ocean.

There are first signs that the geographical ranges of temperate species are shifting northwards (Kraft et al., 2013), while polar fish and ice-associated species are experiencing a reduction in their habitat due to changing environmental conditions in the Arctic Ocean. These ecological changes have impact on the entire ecosystem and jeopardize its stability (Meredith et al., 2019). The complex relationship between biodiversity and ecosystem stability, particularly in the Arctic Ocean, remains a poorly understood area. Consequently, the rapid changes in Arctic sea ice and environmental conditions urgently require an improved understanding of the mechanisms governing the resilience and stability of biological processes and ecosystem functions in the Arctic Ocean.

Marine ecosystem functioning and primary production

Within marine ecosystems, primary production is a key service supporting the food web, the survival and growth of marine organisms (Eppley and Peterson, 1979; Lin et al., 2003). The extent of primary production and its species composition has implications on biodiversity, the abundance and community structure at

higher trophic levels, but also carbon sequestration. In the Central Arctic Ocean (CAO), sea-ice algae rather than phytoplankton account for much of the primary production (Gosselin et al., 1997; Fernández-Méndez et al., 2015). This distinct ecosystem feature is supported by a highly productive microalgal community that thrives in sea ice, accompanied by a remarkably diverse heterotrophic community ranging from bacteria to metazoans (Bluhm et al., 2017). These sea ice algae have the potential to initiate pelagic blooms beneath the ice (van Leeuwe et al., 2022). Historically, it was widely accepted that phytoplankton production beneath sea ice in the CAO was negligible (Arrigo et al., 2012). Typically, phytoplankton growth starts mainly within the marginal ice zone in spring, co-occurring with increased solar radiation and meltwater-induced stratification (Clement Kinney et al., 2020). However, over the past three decades, increasing evidence has documented the occurrence of under-ice blooms in the Arctic Ocean, challenging this prevailing view (Strass and Nöthig, 1996; Fortier et al., 2002; Leu et al., 2011; Assmy et al., 2017). Furthermore, phytoplankton in the water column below the ice shows significant differences from the microalgal communities in the sea ice (Hardge et al., 2017). Recent decades have seen a remarkable increase in the abundance of pelagic phytoplankton in the Arctic Ocean, a direct consequence of the ongoing environmental change in the region, leading to an increase in primary production of more than 50% (Arrigo et al., 2015; Lewis et al., 2020; Nöthig et al., 2020). Emerging evidence highlights the potential of biodiversity to enhance the stability of ecosystem processes, particularly in the face of dynamic environmental change (Duffy, 2009; Cardinale et al., 2012; Hooper et al., 2012; Mori et al., 2013). Nevertheless, the underlying mechanisms driving this phenomenon remain a subject of debate and limited understanding (Loreau and De Mazancourt, 2013). The detailed role of microalgal biodiversity in driving these changes and the subsequent implications for higher trophic levels and on the overall ecosystem stability remains elusive. In addition, it remains to be tested to which extent results obtained from controlled experiments or model simulations in restricted environments are applicable to the far more complex, natural ecosystems. In natural ecosystems, species interactions are subject to variation as a function of the system state, which can cause transitions between stable states (Ives and Carpenter, 2007). With nearly 2,000 phytoplankton taxa and over 1,000 ice-associated protists estimated to inhabit the Arctic (Bluhm et al., 2011), the urgency of identifying keystone species within this wealth of microalgal biodiversity that support ecosystem stability is of paramount importance. These species are crucial for primary production and ecological stability and may serve as indicator species for monitoring the consequences of environmental change in Arctic marine ecosystems (Frey, 2017; Barber et al., 2015; Richter-Menge and Farrell, 2013). Techniques are now accessible to monitor and investigate ecosystem dynamics, enabling examination of the impacts of ecological variables on structural stability. Recent findings indicate that high temperatures in natural ecosystems may affect ecological stability, whereas the consequences of alterations to biodiversity remain variable (Zhao et al., 2023). Ecologists use co-occurrence networks (CON) to examine and visualise how species coexist within communities or ecosystems (Priest et al., 2023; Ma et al., 2016). Cross-convergence mapping (CCM) helps to identify causality in complex ecosystems, while energy landscape analysis (ELA) aids in building ecological models that simulate and predict how ecosystems respond to disturbances or changes of the environmental parameters (Sugihara et al., 2012; Suzuki et al., 2020, 2021).

Aims of this study

This study aims at developing a methodology to reveal ecological relationships, identify key species, and determine their long-term resilience using time series data. Additionally, we aim at identifying species that play a crucial role in maintaining stable communities within the Arctic eukaryotic food web. Furthermore, we seek to define keystone species that can serve as indicators for monitoring the consequences of environmental change in Arctic marine ecosystems. Using network analysis techniques like co-occurrence networks and cross convergence mapping, along with energy landscape analysis, our objective is to understand which factors determine the stability of Arctic marine ecosystems. This approach will improve our understanding of the effects of climate change on this fragile ecosystem.

2 METHODS

2.1 Data

Sampling

Samples were collected with McLane Remote Access Samplers (RAS) deployed in conjunction with oceanographic sensors over four annual cycles (August 2016 - August 2020) deployed at $\tilde{3}0$ m depth on long-term moorings at station F4 (79.0118N 6.9648E) of LTER HAUSGARTEN and FRAM in the Fram strait (Soltwedel et al., 2005). The RAS samplers contained 48 sterile bags, each collecting water samples of 500 mL at programmed sampling events every two weeks. The samples were preserved by adding 700 µl of mercuric chloride (7.5% w/v) to the bags prior to sampling. The samples collected from 2016 to 2018 reflects the pool of up to two samples collected one hour apart in two individual bags. Since 2018, samples from two consecutive weeks have been pooled. Following RAS recovery, water samples were filtered onto Sterivex filter cartridges with a pore size of 0.22 µm (Millipore, USA). Filters were then stored at -20°C for later processing.

Mooring and satellite data

Temperature, salinity and oxygen concentration were measured with a CTD-O_2 attached to the RAS. Physical oceanography sensors were manufacturer-calibrated and processed as described under (von Appen, 2017). Raw and processed mooring data are available at PANGAEA `https://doi.org/10.1594/PANGAEA.904565`, `https://doi.org/10.1594/PANGAEA.940744`, `https://doi.pangaea.de/10.1594/PANGAEA.941125` and `https://doi.org/10.1594/PANGAEA.946447`. For chemical sensors, the raw sensor readouts are reported. The fraction of Atlantic and Polar Water were computed following (von Appen et al., 2018) for each sampling event and reported along with distance below the surface (due to mooring blowdown). Sea ice concentration derived from the Advanced Microwave Scanning Radiometer sensor AMSR-2 (Spreen et al., 2008) were downloaded from the Institute of Environmental Physics, University of Bremen (`https://seaice.uni-bremen.de/sea-ice-concentration-amsr-eamsr2`). Sentinel 3A OLCI chlorophyll surface concentrations were downloaded from `https://earth.esa.int/web/sentinel/sentinel-data-access`. For all satellite-derived data, we considered grid points within a radius of 15km around the moorings. Surface water Photosynthetically Active Radiation (PAR) data, with a 4 km grid resolution, was obtained from AQUA-MODIS (Level-3 mapped; SeaWiFS, NASA) and extracted in QGIS v3.14.16 (`http://www.qgis.org`).

Similar to (von Appen, 2017), the analyzed datasets consist of eigth environmental values for location F4 from 01.08.2016 to 31.07.2020. From this dataset we retrieved the following variables: mixed layer depth (MLD m), water temperature (temp °C), polar-water fraction (PW_frac %), fluorescence chlorophyll concentration from in situ sensor (chl_sens $\sim \mu$g l^{-1}), PAR (μ mol photons $m^{-}2d^{-}1$), Salinity (PSU), O_2 concentration (O2_conc μmol l^{-1}) and water depth (depth m).

After DNA extraction and sequence analysis (see Section 4), we normalised raw counts for CON and CCM using the Hellinger transformation.We do not apply the Hellinger transformation to the energy landscape analysis, hence a different normalisation is introduced in the framework ((Suzuki et al., 2021)).

2.2 Co-Occurrence Network

The abundance of species over the full observation period was converted into temporal profiles by employing Fourier transformation techniques to time-series signals. These temporal profiles rely on the 14 Fourier coefficients. We chose 14 coefficients because they reflect the majority of observed species abundance peaks within the four years. To investigate the similarity of temporal profiles between species pairs, we performed pairwise correlations between the individual temporal profiles. Pairs with 0.7 ($p<0.05$) Pearson correlation were then visualised in an undirected graph. Only positive correlations were retained to later focus on co-operative relationships. Node pairs that have a higher Pearson correlation value show also a similar temporal profile. To identify the various strongly connected components that reflect the existing communities of co-occurring species, we applied the Louvain community detection algorithm (Blondel et al., 2008) on the entire graph. The entire process was implemented using the `CCM` and `networkx` packages in Python; visualization was performed using Cytoscape with the Edge-weighted Spring-Embedded Layout

(Shannon et al., 2003). The whole co-occurrence network construction is described in the Supplements Section 4 Co-Occurrence Network.

2.2.1 Distance between Clusters

To measure the distance between previously defined Louvain communities (clusters), we applied UMAP on time signals obtained after Fourier decomposition of the abundance data. From this we generated a three-dimensional embedding space. Centroids for each cluster were calculated within this space (see Section 4 Figure S2,S3,S4). The network distance between clusters was determined as the Euclidean distance between their centroids. Subsequently, a distance matrix was created and distances were rounded to integers, with only significant connections retained in the pruned matrix.

2.3 Convergent Cross Mapping

Convergent Cross Mapping (CCM) is a method for analysing potential causal relationships between variables in time series data. It attempts to determine whether changes in one time series are associated with changes in another time series. In a first step we built a CCM network from all pairwise combination comprising all species abundance data. Secondly we extracted from this full connected CCM the in- and outgoing edges between the nodes that are connected in the co-occurrence network. We used the implementation of Normalized Mutual Information (NMI) from `https://github.com/polsys/ennemi` by Petri Laarne and the Convergent Cross Mapping by Implementation from Javier, Prince `https://github.com/PrinceJavier/causal_ccm` (Javier et al., 2022) to measure the strength of the causal relationship considering also non-linear relations. We could show that the implementation of Normalized Mutual Information (NMI) results into similar findings as the original implementation based on Pearson correlation (Veilleux, 1979; Sugihara et al., 2012) Section 4.

Using a permutation approach ((Ma et al., 2016)) on the connectivity of the network we defined significance values for the edge weights and investigated whether the current co-occurrence edges exhibit greater NMI values in comparison to random and hypothetical edges Section 4. The whole Convergent Cross Mapping network construction and validation are described in the Supplements Section 4 Convergent Cross Mapping.

2.3.1 Aggregation on cluster level

We enhance the comprehension of inter-cluster interactions by consolidating edges from nodes in Cluster A to Cluster B. We use the arithmetic mean of normalized mutual information (NMI) for this consolidation. This process effectively reduces the number of items in the node cloud, representing clusters through a unified composite node.

After identifying seasonal variations in the microbial clusters through correlation analysis, our research shifts its attention towards identifying stable sub-communities within the clusters. We define a stable consortium of species if they fall within a energetic favourable state under certain environmental condition. In the context of energy landscape analysis, ”energy” represents the potential or stability of different states within a system, such as a biological community. It helps describe how favorable or stable a particular configuration of the system is, with lower energy states being more stable and higher energy states being less stable. Stable states are ecologically significant because they represent the prevailing conditions under which a community operates and the roles of different species within that community. Understanding the existence of stable states and how they can change in response to larger environmental shifts is crucial for comprehending the resilience and adaptability of ecosystems in the face of various ecological challenges. Our objective is to precisely pinpoint keystone species candidates that serve as representatives of these sub-communities, denoting their energy-efficient and consistently stable states.

2.4 Energy Landscape Analysis

The following definitions and algorithms are based on (Suzuki et al., 2021; Fujita et al., 2023). Energy landscape analysis investigates the topological and connectivity characteristics of an energy landscape.

In the supplementary materials (see Section 4 Energy Landscape Analysis), we review the basic concepts of ELA and how it can help assign stable community composition. We use this framework to analyse seasonal clusters obtained by CON, aiming to identify stable communities specific per cluster. In this study, we examined the Energy Landscape using specific parameters and thresholds for occurrence and abundance (described in Section 4 Energy Landscape Analysis). Our analysis focused on the Top 100

ASVs within each cluster. Additionally, it's important to note that outliers were excluded solely for the purpose of plotting.

2.4.1 Estimating stability of communities in different environments

To calculate the energy landscape and the stable states for the communities, we use the following three interaction parameter: i) $\mathbf{J}$ which denotes the interaction between species ii) $\mathbf{G}$, which represents the interaction between species and environment, and iii) the vector h which contain the effects of unobserved environmental factors.The median conditions for the time period of interest (either Arctic Summer or Arctic Winter) represent the environmental data of a specific season. This vector is employed in the calculations of the Energy Landscape Algorithm (ELA). When projecting these calculations to the Arctic, we make assumptions based on the environmental vector given in Table 1. Subsequently, we aim to integrate the predicted stable community species into the time series data of polar regions and assess the impact on the overall species abundance. We simulated only winter and summer, specifying clear external conditions like no light and high polar water influence. The transition phases, like spring and autumn, are too variable in environmental conditions to set fixed parameters.

Table 1. Environmental Parameters for Arctic Summer and Winter

Parameter	Description	Summer	Winter
MLD	Mixed Layer Depth [m]	0	0
PAR	Photosynthetically Active Radiation [μ mol photons $m^{-}2d^{-}1$]	40	0
Temp	Temperature [°C]	-2	-2
Salinity	Salinity [PSU]	34	34
PW_Frac	Precipitable Water Fraction [%]	1	1
O2_conc	Oxygen Concentration [μmol l^{-1}]	350	305
Depth	Depth [m]	30	40

2.5 Keystone Species Definition

After collecting attributes from a co-occurrence analysis and distinguishing between mutualistic influence and occurrence just by chance, we calculated the stable states for different clusters using ELA. This information was merged to define keystone species. We defined a keystone species with: i) a significant influence on other organism in the network (significant NMI value), ii) a high centrality (closeness) value within its co-occurrence community and iii) it was found at least once in a stable state as predicted by the energy landscape algorithm. A significant high centrality value was determined by comparing each centrality value of a single node to the average centrality values of all nodes from the graph using a one sided, one-sample t-test with Benjamini-Hochberg correction for multiple testing (similar to (Guimera and Nunes Amaral, 2005; Joyce et al., 2010).

2.6 Season Definition

The Arctic can be categorized in various ways. For the purposes of this study, we have defined the seasons as follows, based on the availability of light, the seasons and the light.

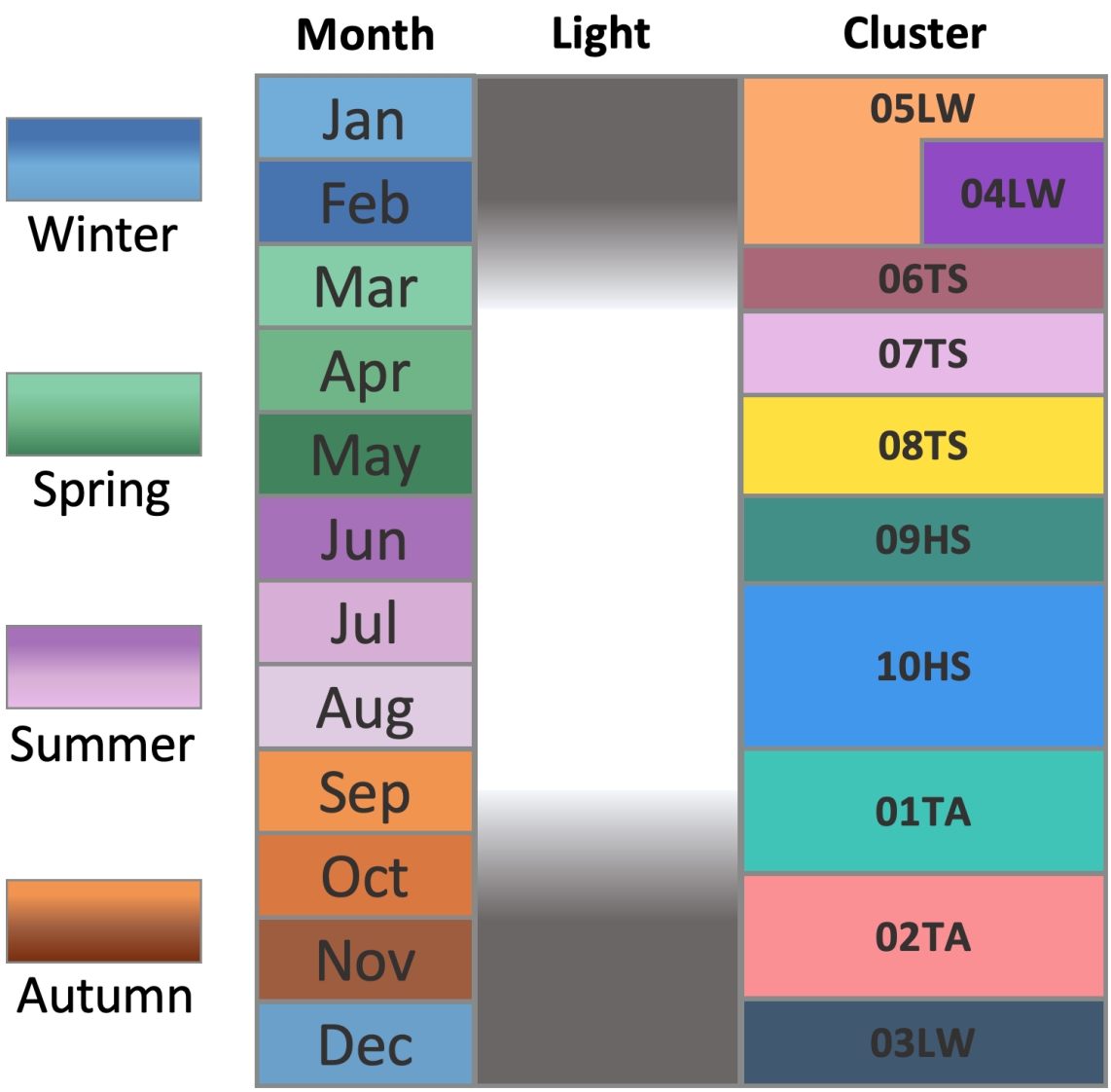

Figure 1. Cluster definition: The names of the cluster are based on the light availability, categorised in transition areas between dark and light(T), high light (H) and low light (L) and the season spring (S), summer(S), autumn (A) and winter (W). Each season consist of three months.

3 RESULTS

We examined a dataset of 1,019 eukaryotic ASVs and eight environmental parameters compiled over four years at mooring site F4 in the West Spitsbergen Current (WSC) in Fram Strait. The aim was to characterize species communities, analysing causal relationships between ASVs and to identify keystone and resilient species with respect to the impact of various environmental conditions.

To accomplish this, we established a novel computational pipeline co-occurrence analysis coupled with convergence cross mapping and energy landscape analysis. This allowed us to identify causal interactions among species in a co-occurring community and to identify energetic stable states of ASVs and communities with respect to different environmental conditions.

3.1 Co-Occurrence Network reveals seasonal dynamics

The co-occurrence network (CON) comprised five connected components, with a major component accounting for 905 (99%) of all nodes, which are connected by 8,429 edges. The twelve disconnected nodes were discarded for further analysis. The resulting undirected graph notably displays a clear seasonal cyclic pattern (Figure 2 A).

The network was partitioned using the Louvain community detection algorithm (Blondel et al., 2008), revealing ten discrete community clusters (Figure 2 B) labeled by the season in which the majority of clusters members had their maximum abundance (Table 2). To further group the clusters, we submerge each three month period to one season. Two clusters were assigned to the transition autumn period (01TA and 02TA), three clusters were associated with the low light winter period (03LW, 04LW and 05LW) and three clusters with the transition spring period (06TS, 07TS and 08TS). Finally, clusters 09 and 10 were allocated to the high light summer season (09HS, 10HS).

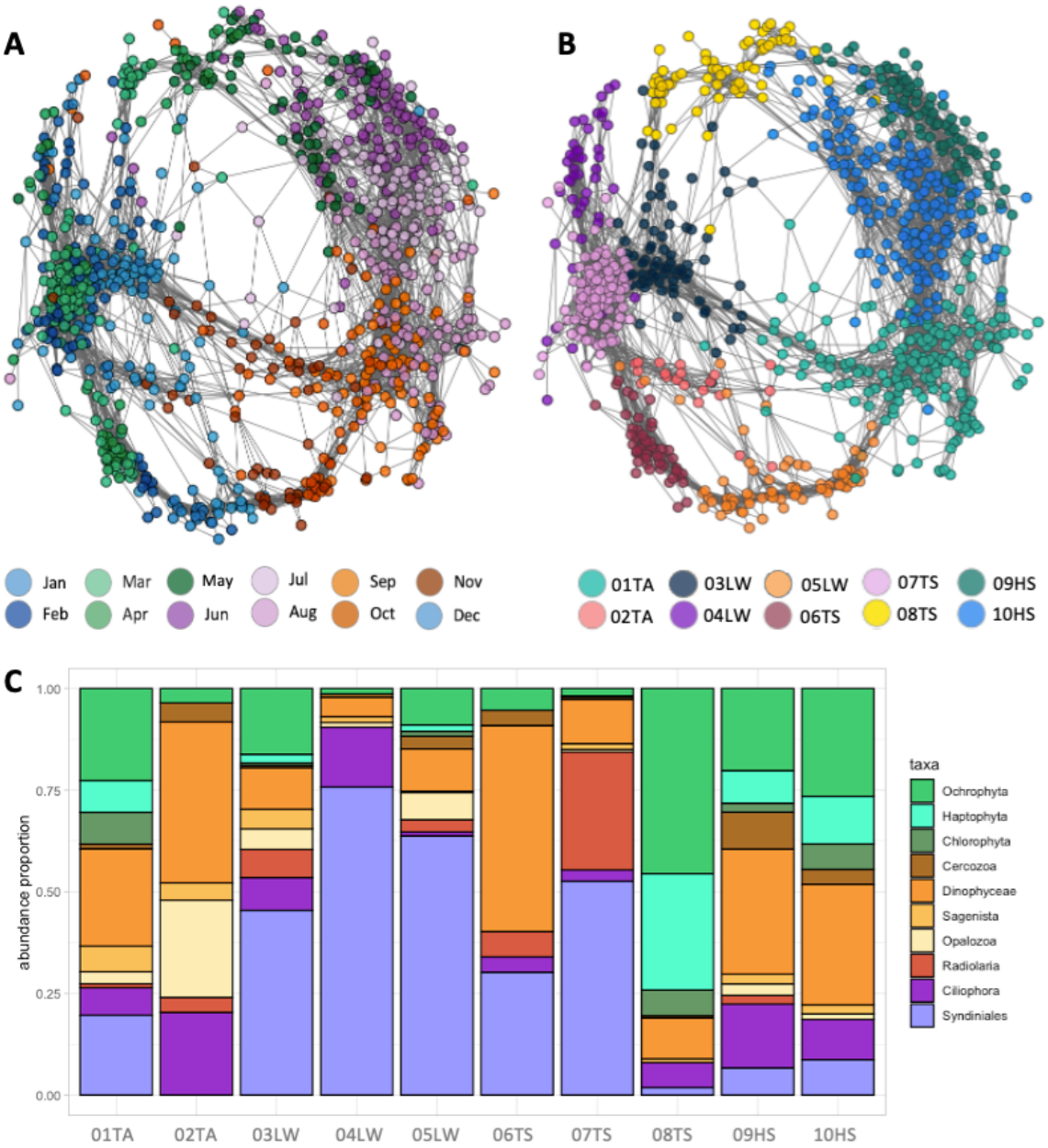

Figure 2. Co-Occurrence Networks of microeukaryots in F4 over a four-year observation period (2016-08-01 to 2020-07-31).
Each network node represents an ASV, and each edge represents a similar temporal pattern of two ASVs. The edge weights correspond to the Pearson correlation coefficients determined from the comparison of the individual ASV temporal profiles. ASVs are connected if the coefficient is $r > 0.7, p < 0.05$. **A:** Node color reflect the month in which the ASV exhibit maximal abundance, calculated from the maximum abundance mode for each year ranging from January to December. **B:** In this representation, nodes are coloured based on the community membership that was determined by the Louvain community detection algorithm. **C:** The relative abundance of the top 10 taxonomic classes. We determine the proportion of the total top 10 taxonomic classes (”Ochrophyta”, ”Haptophyta”, ”Chlorophyta”, ”Cercozoa”, ”Dinophyceae”, ”Sagenista”, ”Opalozoa”, ”Radiolaria”, ”Ciliophora”, ”Syndiniales”), of ASVs within the seasonal clusters (’01TA’, ’02TA’, ’03LW’, ’04LW’, ’05LW’, ’06TS’, ’07TS’, ’08TS’, ’09HS’, ’10HS’). Specifically, the HS’ labels denote high light summer clusters, ’LW’ represents low light winter clusters, ’TS’ corresponds to transition spring clusters, and ’TA’ indicates transition autumn. The percentage of relative abundance is expressed, and the colour gradient visually represents the assignment to either auto- (green), hetero (orange) or mixotroph (purple).

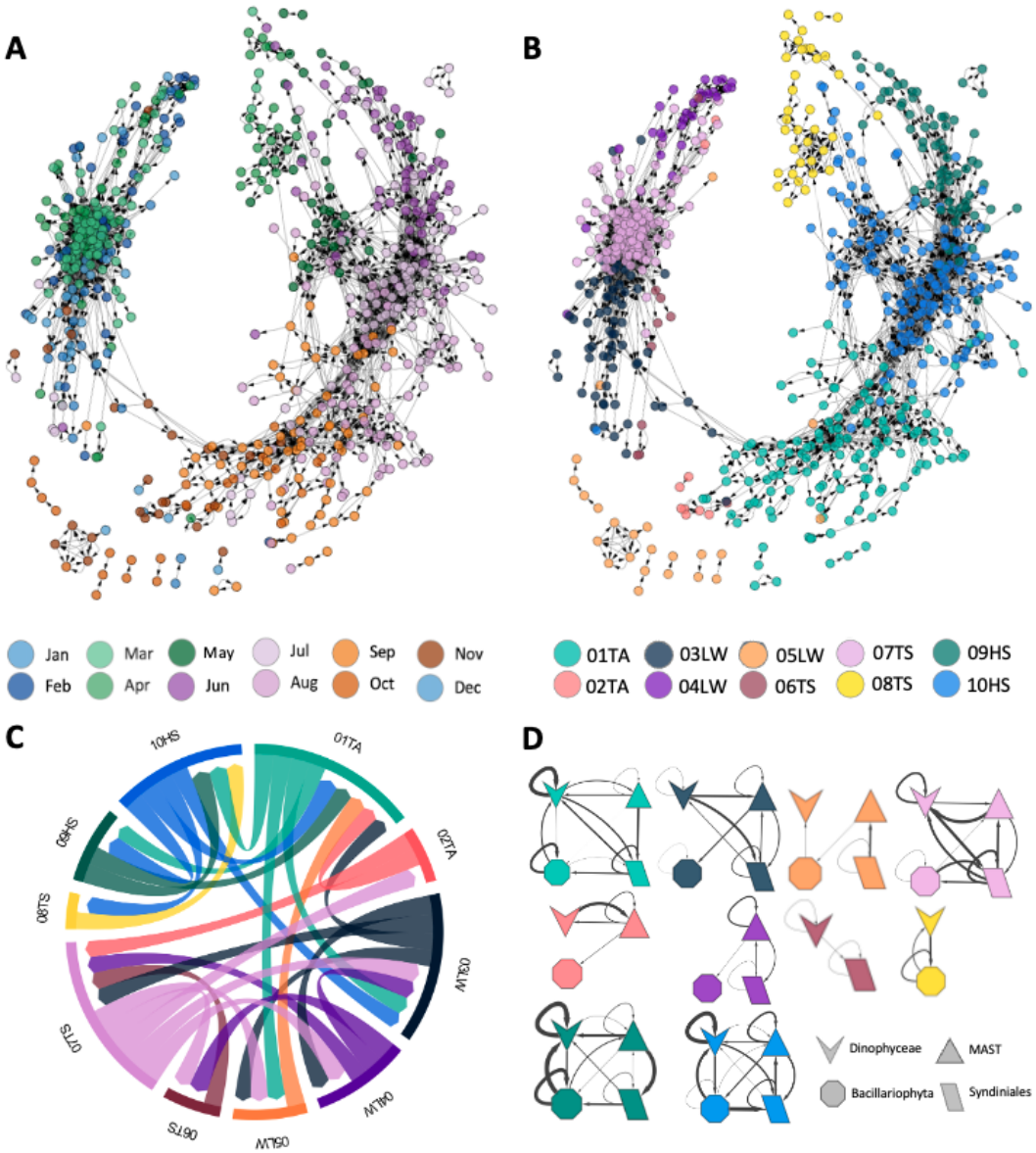

Figure 3. Convergence Cross Mapping Networks of phytoplankton in F4 over a four-year observation period (2016-08-01 to 2020-07-31).
Each node in the CCM network represents an ASV, and each edge represents the similar temporal pattern. The edge weight correspond to the normalized mutual information determined from the comparison of the individual ASV and their predicted representation in the shadow manifold. ASVs are connected if the smoothed p-value of the weight is $p < 0.05$. **A:** Node color reflect the month in which the ASV exhibit maximal abundance, calculated from the maximum abundance mode for each year ranging from January to December. **B:** In this representation, nodes are coloured based on the community membership that was determined by the Louvain community detection algorithm. The ten clusters are illustrated, labelled according to the specific seasonal period, labelled as '01TA', '02TA', '03LW', '04LW', '05LW', '06TS', '07TS', '08TS', '09HS', and '10HS'. In particular, 'HS' labels denote high light summer clusters, 'LW' represents low light winter clusters, 'TS' corresponds to transition spring clusters, and 'TA' indicates transition autumn clusters. **C:**The normalised mutual information aggregated across the edges between the clusters, visually represented by thickness of the arrows corresponding to their respective values. Corresponding colour visually represent the clusters. **D:** Interaction analysis between taxonomic clusters. For each of the ten clusters, the interactions between ASV groups are examined at the taxonomic class level, considering four taxa ('Syndiniales', 'Dinophyceae', 'Bacillariophyta', 'MAST'). The cluster assignments are marked by different colors. The thickness of the arrows denotes the strength of the interaction, while the shapes represent the various taxa groups at the class level.

Table 2. Co-occurrence network clusters. The table shows the ten labeled clusters with their assign season based on month in which the ASV exhibit maximal abundance, calculated from the maximum abundance mode (majority vote) for each year ranging from January to December, the number of ASVs per cluster, and the number of significant edges in network graph.

Cluster	MaxMonth	Season	NumberOfAsv	NumberOfEdges
01TA	9	Autumn	168	1024
02TA	11	Autumn	20	78
03LW	12	Winter	75	509
04LW	2	Winter	45	166
05LW	12	Winter	73	466
06TS	3	Spring	50	382
07TS	3	Spring	154	3062
08TS	4	Spring	62	260
09HS	6	Summer	83	492
10HS	7	Summer	175	1113

3.2 Community-Composition

We explored the taxonomic community per cluster to explore the seasonal associations of each specific taxonomic group. Alpha biodiversity, measured by Shannon entropy, decreases from summer through fall and winter, gradually decreasing towards spring (Section 4 Figure S5). The beta biodiversity score between the winter and spring clusters 06TS is notably lower than the most other scores, except 01TA and 10HS. Cluster 02TA exhibits on average a higher beta diversity compared to all other clusters, which can be explained by the fact that 02TA is the smallest cluster in terms of the number of ASVs (Section 4 Figure S6). In our study, we found distinct taxonomic compositions within various clusters, exhibiting a tripartite division of those taxa into nearly three groups. Photosynthetic organisms like Ochrophyta and Haptophyta dominate the light phases within clusters 08TS to 09HS and 10HS. Initially dominated by autotrophs (exceeding 75%) during the light phase, their abundance gradually decreases but remains above 25%. However, mixotrophs take over during the transition to the dark phase, specifically in clusters 02TA and 03LW. During the dark phase, the dominance of heterotrophs, particularly those from the Syndiniales clusters 04LW, 05LW, and 06TS, becomes evident. The overlay of dark and light in 06TS witnesses a resurgence of Mixotrophs, highlighting the nuanced trophic dynamics during the diurnal cycle. This comprehensive analysis at taxa level provides insights into the composition of these clusters, shedding light on the prevalence and distribution of specific classes within distinct seasonal communities (Figure 2 C).

3.3 Convergent Cross Mapping identifies Community Interactions

To investigate the mutual influence between ASVs, we applied Convergent Cross Mapping (CCM). This method allows predicting causal relationships within and between seasonal clusters based on the underlying ASV dynamics. We project the weights derived from Convergent Cross Mapping (CCM) onto the co-occurrence network, resulting in a directed graph consisting of directed 16,858 edges and 905 nodes. Here, a directed edge indicates that knowledge of the dynamics of the source node allows for prediction of the dynamics of the target node.

A comparative analysis of edge weights within the Convergent Cross Mapping (CCM) network was conducted. The connectivity derived from the co-occurrence network was compared with theoretical edge weights and randomly permuted connections. To perform this comparison, a two-sided Kolmogorov-Smirnov test was used. The theoretical edge weights were derived from all possible connections between pairs of nodes in the co-occurrence network, excluding the existing true links (Section 3.3). The findings clearly show that there is a stronger mutualistic influence (higher NMI values) between co-occurring species compared to random or to unconnected nodes (Section 4 Figure S8 and S9 and Table S1 and S2). The significance level was set at a nonparametric p-value of less than 0.05 calculated similar to Ma et al. (2016). Trimming edges with non-significant NMI values (Section 4 Figure S10), produced a network graph consisting of 3,654 edges and 637 nodes, divided into 14 disconnected components, with the largest module encompassing 603 nodes (Fig. 3 A,B).

In contrast to the co-occurrence pattern, the apparent interrelation patterns revealed by CCM indicates a disrupted seasonal cycle within the network structure. In the context of the CCM Network, ”disintegrate” refers to removing edges with insignificant weights. Of the total 13,204 edges eliminated, 18.79% represent connections between species reaching their peak abundance in March. This selective removal has a profound impact on the network structure, (Figure 3 A). Due to the disintegration, the network breaks during spring season, resulting in two separate springs, as demonstrated in Figure 3 A (months March and April). The winter cluster 05LW and the spring cluster 06TS collapse, as shown in Figure 3 B. The collapse pertains to the separation and disintegration of nodes in particular clusters from the overall network structure. This suggests that these connections are not a result of causal interactions, but rather result from simple co-occurrence, possibly caused by the prevailing environmental conditions. Analysis of the betweenness centrality reveals that species of Picozoa, Leegaardiella, Acantharea, Dinophyceae, MAST-1, and Syndiniales serve as essential hub nodes throughout the seasonal cycle in the network, highlighting their crucial function in maintaining network stability.

3.4 Community Interaction

Analyzing cluster interactions revealed distinct patterns. We measure distance of clusters by ”network distance”, a metric designed to evaluate the separation between clusters. This measure is computed by assessing the distance between the centroids of clusters within the dimension-reduced UMAP embedding space (Section 3.3). Distances between clusters thus determined range between 1 and 8. Proximate clusters (a network distance of two to four), exhibited notably higher connectivity compared to clusters situated further apart (distance five to eight). Figure 3 C provides a visual and quantitative representation of these interactions. Subsequent analysis revealed a prevalence of connections at a network distance of two (44% of total connections), followed by distances of three (29% of total connections), and four (26% of total connections)(Section 4 Figure S2,S3,S4).

The average effects of two linked clusters revealed that summer has a greater influence on winter than the inverse association. This suggests that predicting which organisms will be present in winter, based on the knowledge of the organisms prevalent in summer, is more reliable than the reverse prediction. The summer biomass is a precursor for winter, but not the other way around (Figure 3 C).

We could reconstruct the mutualistic influence between all pairs of the four different seasonal phases with one exception: from low light associated species no significant link to high light members could be reconstructed (Figure 3 C).

In our investigation, we combined ASVs into four taxonomic groups selected from the top ten classifications (Figure 2 C): Bacillariophyta, Syndiniales, Dinophyceae, and Mast (MArine STramenopile; all Mast-X variants were classified under Mast) (Figure 2 C). Bacillariophyta primarily comprises photo-autotrophic species (Mann et al., 2017), while Syndiniales include species with parasitic tendencies, most of them characterized by their heterotrophic lifestyle (Suter et al., 2022). Dinophyceae, another key group within our analysis, is known for its diverse array of species with varying ecological roles, from symbionts to planktonic autotrophs (Lin et al., 2022). MASTs are heterotrophic protists and contribute substantially to protist abundances in the ocean. They play a crucial role in marine ecosystems and are one of the dominant eukaryotes in the Arctic Ocean (Thaler and Lovejoy, 2014; Lin et al., 2022).

These four taxonomic groups are primarily distinguished by their unique lifestyles and ecological roles as primary producers, consumers, parasites, or endosymbiotic interactors. These distinctions form the basis for our analysis of their contributions to the ecosystem. Hence, by summarizing the members of each group into single nodes, we analyzed their cross-interactions using the information obtained from the CCM network.

This analysis revealed that the strength and direction of interactions between these taxonomic groups varied over the annual cycle. Notably, during the spring-summer and summer-fall transition periods, clusters 02TA and 06TS displayed fewer and weaker connections compared to other clusters. This suggests dynamic changes in community structure during these periods, with ecological interactions between individual species either yet to be established or no longer present. At the start of the polar night (cluster 03LW), we detected the most substantial influence from the dinoflagellates (shown by the thickest arrow in Figure 3 C) to the pico-eukaryotic heterotrophic groups Syndinales and MAST, suggesting a crucial ecological role of dinoflagellates for the establishment of the winter community. Overall, the strength of the links between the taxonomic groups decreases as the polar night progresses and has its minimum at the peak of the polar

night in December (Cluster 05LW). The lack of strong connections between taxonomic groups during the deepest polar night indicates that there are only a few ecologically significant interactions within the eukaryotic microbial community.

During the polar day, as the sunlight becomes more intense, the connections between taxonomic groups become stronger and reach their peak during the zenith of the polar day (Cluster 10HS). Notably, the Bacillariophyta group shows the most robust connections during the polar day. This group, comprised of diatoms, plays a critical role as the leading phototrophic biomass producer and forms the foundation of the marine food web. However, towards the end of the growth period, the impact of MAST on Dinoflagellates becomes more pronounced (as shown by the thicker arrow), indicating an essential involvement of this pico-eukaryotic heterotroph in the ecosystem during the later growth phase. This is also a signature of the transition from primary production to recycling.

3.5 Community and Environment Interactions

For a more detailed understanding of which environmental conditions align with seasonal community clusters, we conducted a correlation analysis (Figure 4). Cluster 10HS displayed a significant positive correlation with Photosynthetically Active Radiation (PAR) (0.67) and temperature (0.49), but a significant negative correlation with Mixed Layer Depth (MLD) (-0.61). This cluster thrives in environments with high light and temperature levels but less deeper mixed layers. Cluster 03LW exhibits the opposite behavior, showing a moderately positive correlation with MLD (0.23) and polar water fraction (PW_frac) (0.24) while displaying an inverse relationship with PAR and temperature (-0.35 and -0.36, respectively).

3.6 Energy Landscape Analysis determines stability of microbial communities

Energy landscape analysis provides a map of the challenges and opportunities present in different community compositions. This helps us understand how organisms adapt to their environment and visually see the pathways that lead to different community compositions.

To conduct the energy landscape analysis, we focused on the 100 most abundant types of microorganisms (ASVs) in each cluster.

We used energy landscape analysis to explore stable states in the multidimensional space of community structure. This involved analyzing time-series data from microbiomes, as described in Suzuki et al. (Suzuki et al., 2021).

In our study, we introduced changes in environmental conditions over time, assuming that each of the ten clusters had a flexible ”energy landscape” for community states.

We observed shifts between these stable states, which were caused by changes in variables like the population density of microbial ASVs. These shifts are evident in Figure 1c, where ASVs influence each other, and they resemble ”regime shifts” described in previous studies (Scheffer et al., 2001; Scheffer and Carpenter, 2003; May, 1977). These transitions require the reorganization of the energy landscape, primarily driven by changes in environmental factors such as temperature or light.

The persistence of a single stable state throughout each season suggests a consistent response to prevailing environmental factors, including temperature, nutrient availability, and species interactions. This underscores the ecological adaptability of these clusters to specific seasonal conditions. This niche specificity is also highlighted in Figure 4. Here it is clearly visible that each cluster correlates only with specific environmental parameters.

By analyzing the four-year dynamics of each cluster, we have deduced the existence of several stable states (Figure 5, Table 3). The number of stable states varies between clusters, with autumn and winter clusters having on average more stables states (e.g. cluster 01TA with five stable states) compared to summer and spring clusters.Using statistical physics methods (Watanabe et al., 2014; Suzuki et al., 2021; Becker and Karplus, 1997), community dynamics can be divided into phases wherein they fluctuate around nearby balance points and phases wherein they transition into nearby equilibria. In the presence of multiple equilibrium points (Figure 5), observed phytoplankton dynamics cannot be adequately explained by transient dynamics converging onto a single equilibrium point.

Figure 5 illustrates a cluster for each season. The data reveal that communities in cluster 08TS and 03LW maintain a consistent energetic state over the entire period, while in cluster 01TA it is clearly visible that

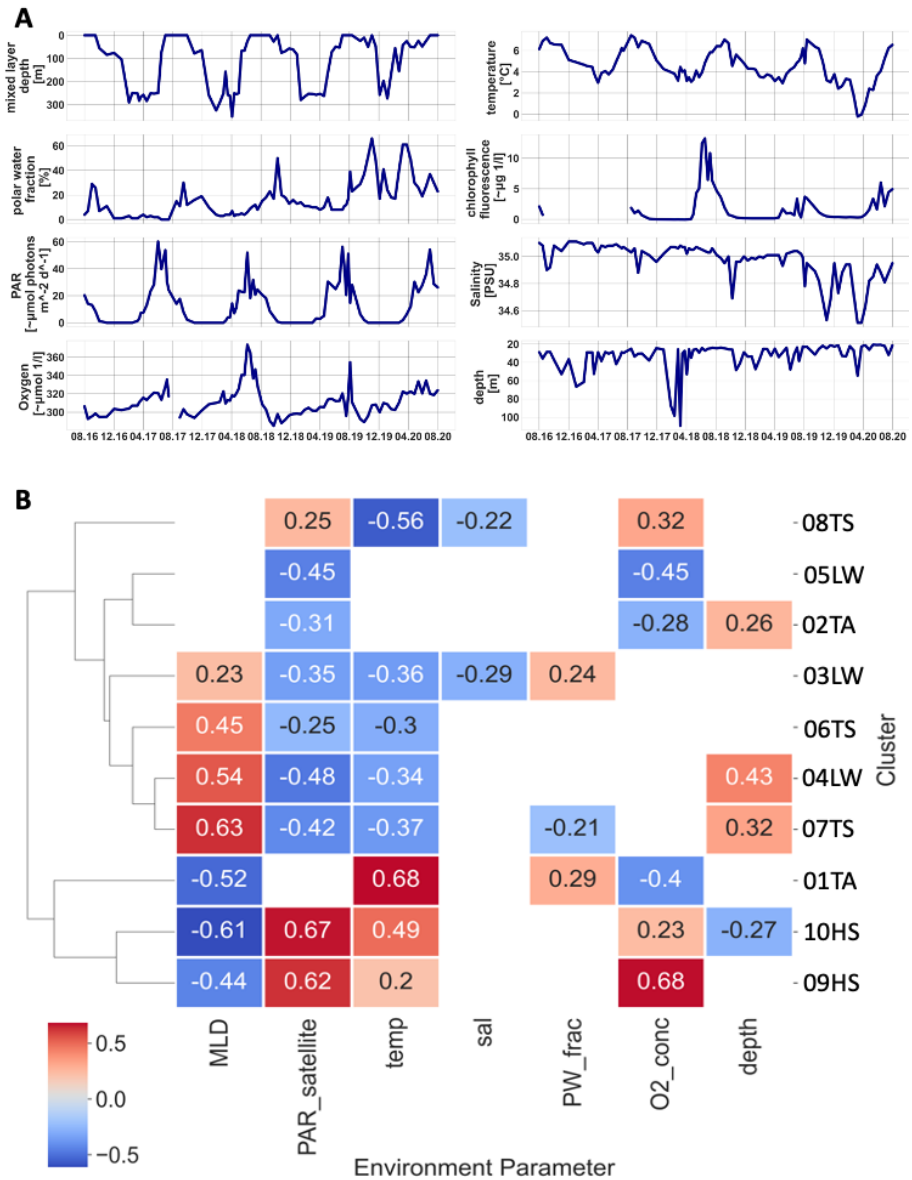

Figure 4. Environmental data and correlation with the seasonal clusters. A): Environmental data for F4 (dark blue) over a four-year observation period (2016-08-01 to 2020-07-31). The x-axis represents the time period, while the y-axis indicates the following parameters: Mixed Layer Depth (MLD) [m], Temperature [°C], Chlorophyll Fluorescence [μ g/L], Polar Water Fraction [%], Photosynthetically Active Radiation (PAR) [μ mol photons/m^2/d], Salinity [Practical Salinity Units (PSU)], Oxygen Concentration [μ mol/L], Depth [m]. **B): Correlation analysis was conducted to determine the relationship between environmental parameters and seasonal clusters.** The displayed chart shows the environmental parameters from section a) in relation to seasonal clusters. These clusters are characterized by the cumulative relative abundance of ASVs. Cluster labels include '01TA', '02TA', '03LW', '04LW', '05LW', '06TS', '07TS', '08TS', '09HS', and '10HS', where 'TA' denotes transition autumn clusters, 'LW' represents low light winter clusters, 'TS' pertains to transition spring clusters, and 'HS' signifies high light summer clusters. The colour gradient used in the heatmap illustrates the strength of the correlation visually, with blue shades indicating negative correlations and red shades indicating positive correlations. It is worth noting that a significance mask has been applied to show only correlations that are statistically significant.

samples from the fall are energetically most beneficial. Interestingly, cluster 10HS shows a noteworthy energetic gradient, with spring and summer samples being the most energetically favorable, while the

winter and autumn samples require more energy. The cluster of highlights during the summer displays a wider range of energy, where organisms can be observed in the samples. (Figure 5).

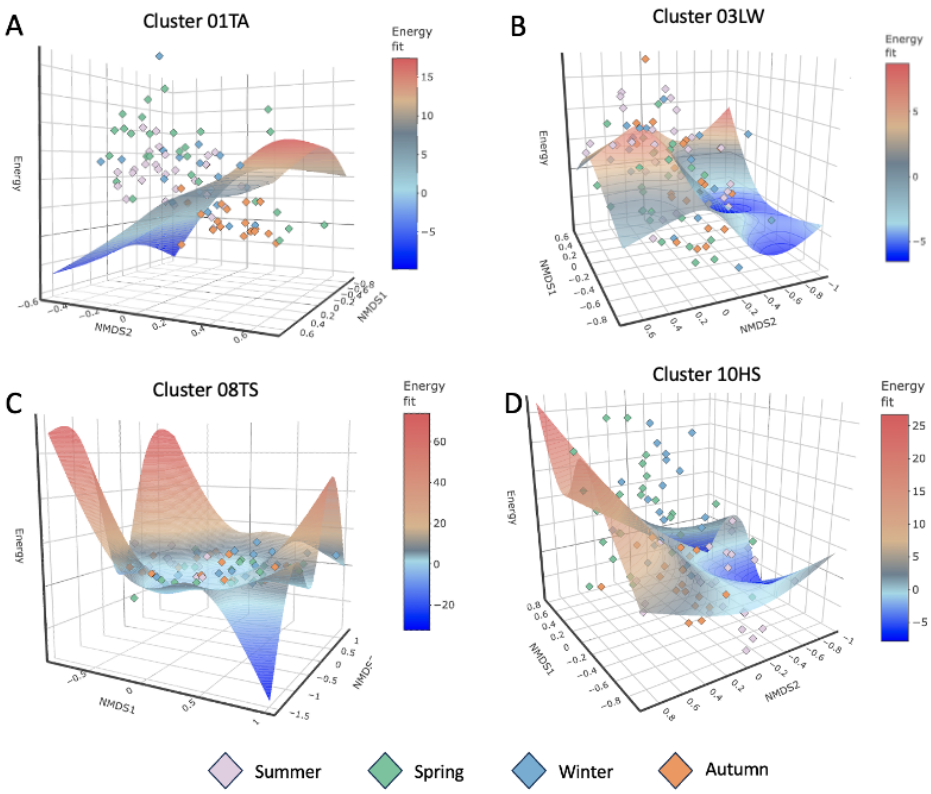

Figure 5. Energy landscapes depicting community structure dynamics. The plots display the reconstructed energy landscape on the NMDS surface for a cluster of each season. Community states, which are defined by ASV compositions and occupy lower-energy regions, indicate higher stability within the energy landscapes. **A):** The transition autumn cluster 01TA. **B):** The low light winter cluster 03LW. **C):** The transition spring cluster 08TS. **D):** The high light summer cluster 10HS. Environmental landscapes over the NMDS surface are reconstructed for each of the four example clusters. The z-axis displays the energy, while the x- and y-axes display the first and second NMDS dimensions. The landscape contours were estimated using a smoothing spline approach with optimized penalty parameters.

3.7 Characterisation of keystone phytoplankton species in the Fram Strait

A thorough analysis of the co-occurrence network, mutualistic interactions, and energy landscape revealed the existence of 19 keystone species across the complete annual cycle within the measured environmental profile (Table 3). Notably, clusters 09HS and 10HS had high numbers of keystone species, with two and seven, respectively. On the other hand, clusters 03LW and 04LW in low light conditions had a lower number of keystone species, with four and one, respectively. The autumn cluster 01TA harbors four keystone species, whereas the spring cluster 07TS has only one. Remarkably, the taxa from the summer clusters are classified into the following taxonomic groups: five Ochrophyta, two Dinophyceae, and two Ciliophora. These groups include Fragilariopsis, Pseudo-nitzschia, and Thalassiosira, which are known to contribute significantly to the biomass during this season (Von Quillfeldt, 2000). Notably, Fragilariopsis and Thalassiosira exhibit the highest abundance within this cluster. The keystone species taxa in the winter clusters comprise three Syndiniales, one Radiolaria, and one Dinophyceae. The autumn cluster contains two Ochrophyta, one Chlorophyta, and one Syndiniales. Surprisingly, we couldn't predict any keystone species for the spring period indicating that this period could be the most variable and selective one. These 19 keystone species epitomize the ecological roles played by all network members engaged in primary production, consumption, and parasitic interactions. Notably, the emergence of Chlorophyta as a keystone species during the beginning of the autumn period in September suggests a shift in primary production from Ochrophyta to Chlorophyta, species that may prefer colder temperatures for growing (Tragin and Vaulot, 2018).

Table 3. ASV identified as potential keystone species for cluster 10HS, 06TS, 03LW and 01TA. The taxonomic classifications, clusters, raw abundance, proportion of total raw abundance, cluster abundance, and proportion of cluster raw abundance are presented in summary form over the 4-year observation period. The column, significance, indicates if this ASV (Nodes) has at least on significant CCM connection measured in normalized mutual information.

Nodes	Phylum	Genus	Species	Cluster	relAbund	Closeness
euk_asv12	Ochrophyta	Fragilariopsis	Fragilariopsis uc	10HS	0.009	0.356
euk_asv35	Ochrophyta	Fragilariopsis	Fragilariopsis_sublineata	10HS	0.007	0.345
euk_asv24	Ochrophyta	Pseudo-nitzschia	Pseudo-nitzschia_sp.	10HS	0.006	0.312
euk_asv28	Ochrophyta	Thalassiosira	Thalassiosira uc	10HS	0.006	0.317
euk_asv54	Dinoflagellata	Gyrodinium	Gyrodinium_fusiforme	10HS	0.006	0.308
euk_asv52	Dinoflagellata	Peridiniales uc	Peridiniales uc	10HS	0.005	0.345
euk_asv125	Ciliophora	Dadayiella	Dadayiella_ganymedes	10HS	0.003	0.356
euk_asv115	Ochrophyta	Mediophyceae uc	Mediophyceae uc	09HS	0.004	0.284
euk_asv186	Ciliophora	Strombidiidae_H uc	Strombidiidae_H uc_sp.	09HS	0.002	0.313
euk_asv5	Radiolaria	RAD-C uc	RAD-C uc_sp.	07TS	0.014	0.307
euk_asv21	Dinoflagellata	Dino-II-10-and-11 uc	Dino-II-10-and-11 uc_sp.	04LW	0.009	0.291
euk_asv87	Radiolaria	RAD-B-Group-IV uc	RAD-B-Group-IV uc_sp.	03LW	0.002	0.338
euk_asv198	Dinoflagellata	Dino-II-6 uc	Dino-II-6 uc_sp.	03LW	0.001	0.314
euk_asv213	Dinoflagellata	Gymnodinium	Gymnodinium_sp.	03LW	0.001	0.309
euk_asv780	Dinoflagellata	Dino-I-5 uc	Dino-I-5 uc_sp.	03LW	0.000	0.299
euk_asv163	Dinoflagellata	Dino-I-1 uc	Dino-I-1 uc_sp.	01TA	0.003	0.368
euk_asv118	Chlorophyta	Chloroparvula	Chloroparvula_pacifica	01TA	0.002	0.369
euk_asv330	Ochrophyta	Pelagophyceae uc	Pelagophyceae uc_sp.	01TA	0.002	0.326
euk_asv401	Ochrophyta	Aureococcus	Aureococcus_anophagefferens	01TA	0.001	0.315

3.8 Projection of environment conditions from the Central Arctic to Atlantic communities.

Building upon an analysis of sample distribution across various environmental parameters, we manipulated environmental factors to simulate a typical summer and winter day in the F4 (Atlantic Current) region and the Central Arctic. We have limited the simulations to winter and summer, as we are able to specify clear external conditions to observe changes, such as no light and a high influence of polar water. The transition phases of spring and autumn are highly dependent on changing environmental conditions, thus we have refrained from selecting fixed environmental parameters for this period. Employing the ELA model and parameter estimation, we identified theoretically stable states and assessed the associated energy fluctuations. Subsequently, we investigated the presence of these stable ASV components within the

Central Arctic and evaluated their potential for alterations. We subsequently compared the stable states and predicted keystone species from two representative clusters, one from the high light period (10HS) and the other from the low light period (03LW), between the original dataset and the simulated Atlantic and Arctic profiles. As anticipated, we observed subtle differences between the measured Atlantic profile and the simulated one. For instance, while the predicted keystone species for the high light period remained consistent in the simulated dataset, some discrepancies emerged under low light conditions. Notably, one novel heterotrophic Opalozoa species (*MAST-3F*) from Lin et al. (Lin et al., 2022) was identified as stable, along with one Ochrophyte species (*Chrysophyceae H*) and eight additional Syndiniales species (Table 3,Table 4, Figure 6 Figure 6).

The comparison with typical Arctic conditions revealed broader differences under both light and dark regimes. In the Arctic summer cluster (10HS), no Dinophyceae species was identified as a keystone species, and only two Ochrophyta species (*Dictyocha speculum* and *Chaetoceros brevis*) were identified, compared to the four predicted under Atlantic real and simulated conditions. This observation is in line with previous findings, where Chaetoceros species were preferably found under ice (Booth and Horner, 1997). Further, Chaetoceros was found to make a significant contribution to the summer biomass(Crawford et al., 2018). Additionally, this cluster harbored a photosynthetic (Laza-Martínez et al., 2012), Cryptophyta species, *Teleaulax gracilis*. The winter Arctic cluster (03LW) contained one additional Ochrophyte species, two Opalozoa species, one Sagenista (*MAST-9A*) species, and three additional Syndiniales species compared to the original Atlantic conditions (Table 5).

Table 4. (Atlantic) ASV identified as a potential keystone species for clusters 10HS, 03LW projected to the a Atlantic environmental parameters. The taxa, clusters, raw abundance, proportion of total raw abundance and cluster abundance, and proportion of cluster raw abundance are shown aggregated over the 4-year observation period. The column, significance, indicates if this ASV (Nodes) has at least on significant CCM connection measured in normalized mutual information.

Nodes	Phylum	Genus	Species	Cluster	relAbund	Closeness
euk_asv12	Ochrophyta	Fragilariopsis	Fragilariopsis uc	10HS	0.009	0.356
euk_asv35	Ochrophyta	Fragilariopsis	Fragilariopsis_sublineata	10HS	0.007	0.345
euk_asv24	Ochrophyta	Pseudo-nitzschia	Pseudo-nitzschia_sp.	10HS	0.006	0.312
euk_asv28	Ochrophyta	Thalassiosira	Thalassiosira uc	10HS	0.006	0.317
euk_asv54	Dinoflagellata	Gyrodinium	Gyrodinium_fusiforme	10HS	0.006	0.308
euk_asv52	Dinoflagellata	Peridiniales uc	Peridiniales uc	10HS	0.005	0.345
euk_asv125	Ciliophora	Dadayiella	Dadayiella_ganymedes	10HS	0.003	0.356
euk_asv79	Ochrophyta	Chrysophyceae H uc	Chrysophyceae H uc_sp.	03LW	0.002	0.313
euk_asv87	Radiolaria	RAD-B-Group-IV uc	RAD-B-Group-IV uc_sp.	03LW	0.002	0.338
euk_asv198	Dinoflagellata	Dino-II-6 uc	Dino-II-6 uc_sp.	03LW	0.001	0.314
euk_asv213	Dinoflagellata	Gymnodinium	Gymnodinium_sp.	03LW	0.001	0.309
euk_asv411	Dinoflagellata	Dino-II-20 uc	Dino-II-20 uc_sp.	03LW	0.001	0.306
euk_asv476	Dinoflagellata	Dino-II-22 uc	Dino-II-22 uc_sp.	03LW	0.001	0.294
euk_asv553	Dinoflagellata	Dino-II-21 uc	Dino-II-21 uc_sp.	03LW	0.001	0.304
euk_asv615	Dinoflagellata	Dino-II-20 uc	Dino-II-20 uc_sp.	03LW	0.001	0.363
euk_asv803	Opalozoa	MAST-3F uc	MAST-3F uc_sp.	03LW	0.001	0.306
euk_asv1403	Dinoflagellata	Dino-I-5 uc	Dino-I-5 uc_sp.	03LW	0.000	0.316
euk_asv545	Dinoflagellata	Dino-I-2 uc	Dino-I-2 uc_sp.	03LW	0.000	0.288
euk_asv602	Dinoflagellata	Dino-II-9 uc	Dino-II-9 uc_sp.	03LW	0.000	0.329
euk_asv780	Dinoflagellata	Dino-I-5 uc	Dino-I-5 uc_sp.	03LW	0.000	0.299
euk_asv837	Dinoflagellata	Dino-Group-II uc	Dino-Group-II uc	03LW	0.000	0.349

Table 5. (Arctic) ASV identified as potential keystone species for cluster 10HS, 03LW projected to the arctic environmental parameters. The taxa, cluster, raw abundance, proportion of total raw abundance and cluster abundance, and the proportion of cluster raw abundance are shown aggregated over the 4-year observation period. The column, significance, indicates if this ASV (Nodes) has at least on significant CCM connection measured in normalized mutual information.

Nodes	Phylum	Genus	Species	Cluster	relAbund	Closeness
euk_asv132	Ochrophyta	Dictyocha	Dictyocha_speculum	10HS	0.003	0.314
euk_asv161	Cryptophyta	Teleaulax	Teleaulax_gracilis	10HS	0.003	0.299
euk_asv214	Ochrophyta	Chaetoceros	Chaetoceros_brevis_3	10HS	0.002	0.300
euk_asv79	Ochrophyta	Chrysophyceae H uc	Chrysophyceae H uc_sp.	03LW	0.002	0.313
euk_asv87	Radiolaria	RAD-B-Group-IV uc	RAD-B-Group-IV uc_sp.	03LW	0.002	0.338
euk_asv213	Dinoflagellata	Gymnodinium	Gymnodinium_sp.	03LW	0.001	0.309
euk_asv489	Sagenista	MAST-9A uc	MAST-9A uc_sp.	03LW	0.001	0.288
euk_asv547	Opalozoa	MAST-3 uc	MAST-3 uc	03LW	0.001	0.316
euk_asv615	Dinoflagellata	Dino-II-20 uc	Dino-II-20 uc_sp.	03LW	0.001	0.363
euk_asv803	Opalozoa	MAST-3F uc	MAST-3F uc_sp.	03LW	0.001	0.306
euk_asv1088	Dinoflagellata	Dino-II-16 uc	Dino-II-16 uc_sp.	03LW	0.000	0.326
euk_asv1403	Dinoflagellata	Dino-I-5 uc	Dino-I-5 uc_sp.	03LW	0.000	0.316
euk_asv602	Dinoflagellata	Dino-II-9 uc	Dino-II-9 uc_sp.	03LW	0.000	0.329
euk_asv837	Dinoflagellata	Dino-Group-II uc	Dino-Group-II uc	03LW	0.000	0.349

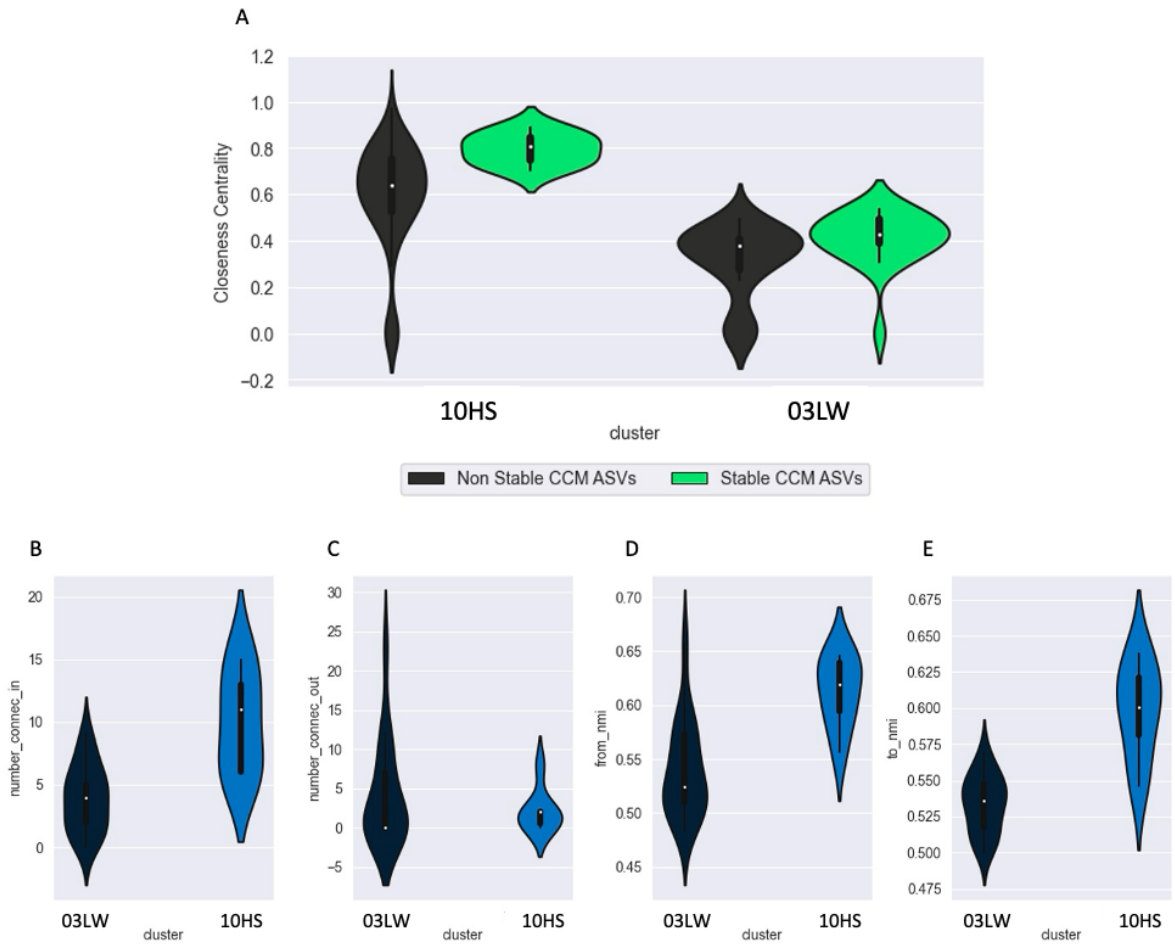

Figure 6. Closeness Centrality for stable state ASV vs non stable state ASVS. A): The Closeness Centrality for stable ASV vs non stable state ASVs. The stable ASVs are indicated with green, and the non stable ASVs are black. **Comparison of connection and interaction for winter and summer. B):** The number of connection from the stable ASV within their cluster. **C):** The number of connection from the stable ASV to other clusters. **D):** The mean over normalized mutual information from the stable ASV to other ASVs. **E):** The mean over normalized mutual information to the stable ASV from other ASVs. More details can be found in Section 4 Table S3 and S4.

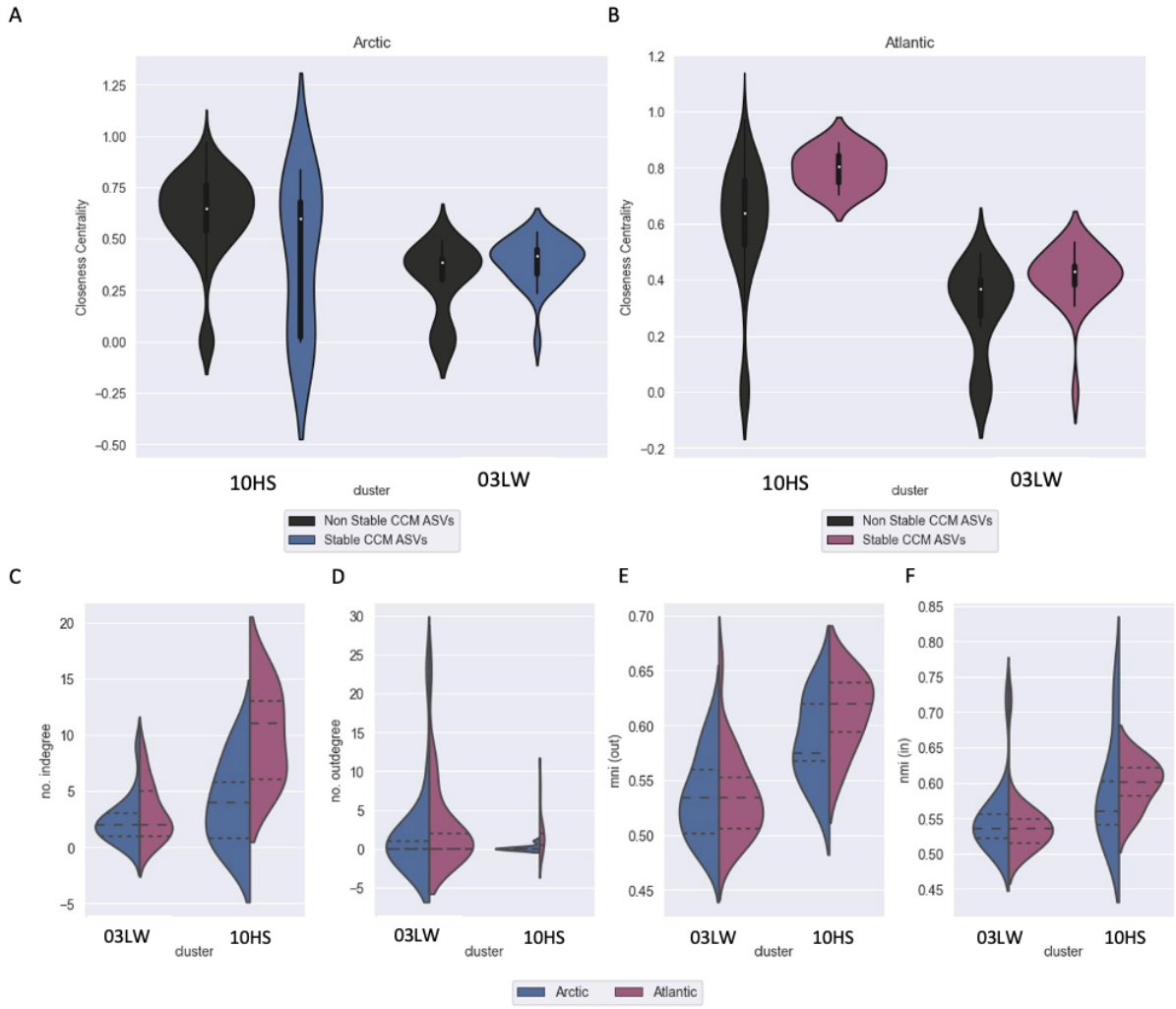

Figure 7. Closeness Centrality for Arctic and Atlantic stable state ASV vs non stable state ASVS. A): The Closeness Centrality for stable ASV for Arctic Environmental condition vs non stable state ASVs. **B):** The Closeness Centrality for stable ASV for Atlantic Environmental condition vs non stable state ASVs. The stable ASVs from the arctic environment are indicated with blue (1), the stable ASVs from the atlantic environment are purple (1) and the non stable ASVs are black (0). **Comparison of connection and interaction for Arctic and Atlantic winter and summer. C):** The number of connection from the stable ASV within their cluster. **D):** The number of connection from the stable ASV to other clusters. **E):** The mean over normalized mutual information from the stable ASV to other ASVs. **F):** The mean over normalized mutual information to the stable ASV from other ASVs. More details can be found in Section 4 Table S5 to S8.

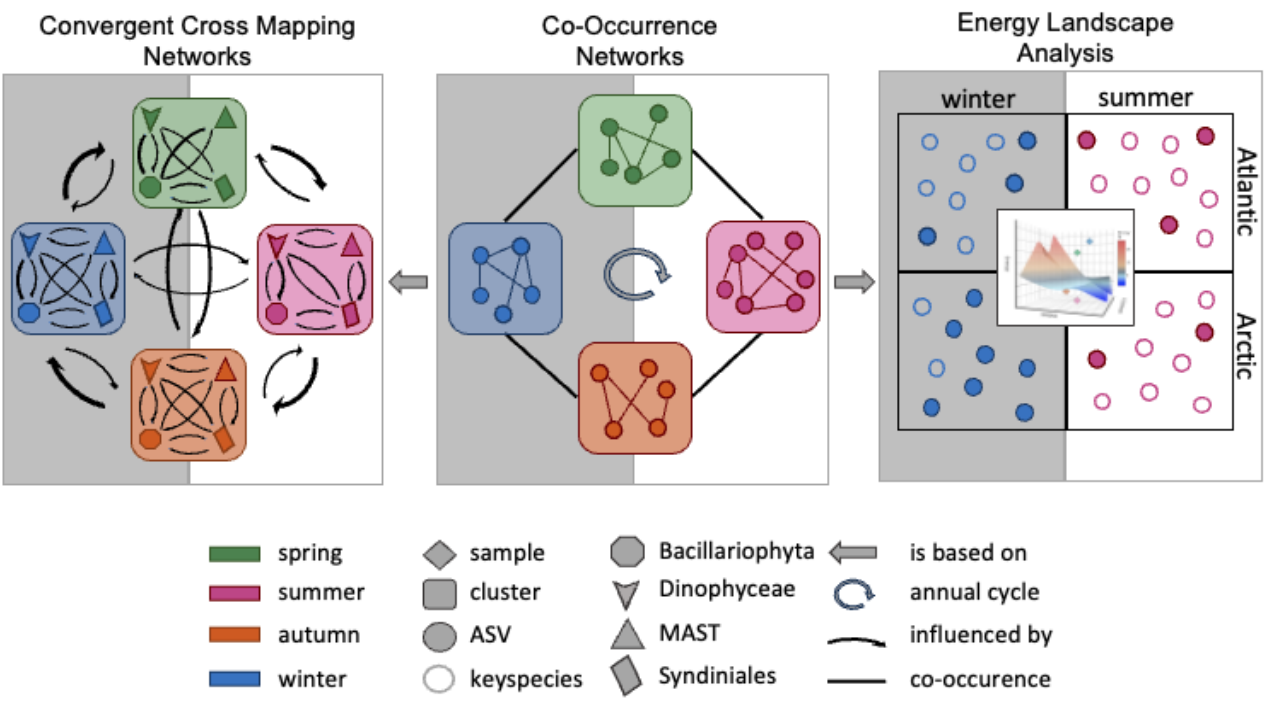

Figure 8. Our Workflow for Identifying keystone species: The middle panel displays the results of clustering achieved through analysis of the Co-Occurrence Network. Each season is presented as a distinct cluster, including spring, summer, autumn and winter. Following this, a Convergence Cross Mapping Network is calculated, based on the connections within the network. It reveals the normalized mutual information score of the four taxonomic class levels within and between clusters, as depicted in the right panel. The taxonomic classes in this study encompass Bacillariophyta (hexogram), MAST (triangle), Syndiniales (parallelogram), and Dinophyceae (V). The ASVs (circles) that represent the samples (diamonds) are organized into seasonal clusters for an Energy Landscape Analysis. keystone species are identified based on their occupancy within Stable States (rings) in the left panel. Finally, the last panel shows the stable sets that correspond to the typical habitats during winter and summer in the Arctic and Atlantic regions, determined by assessing the abundance of our Atlantic communities. The dark gray background represents low light conditions, while the white background indicates high light periods.

4 DISCUSSION

In this study, we developed a new method of investigating ecological time series data using amplicon derived abundance information, by combining three data analysis methods: Co-Occurrence Networks (CON) (Stephens et al., 2009), Convergent Cross Mapping (CCM) (Sugihara et al., 2012), and Energy Landscape Analysis (ELA) (Suzuki et al., 2021). By integrating three methodological approaches, we aimed to identify and characterize keystone species in the Arctic across different seasons. In addition, we examine how these keystone species are effected by changing environmental conditions, including global warming and Arctic atlantification. We also investigate how these keystone species affect other organisms, and how their effects vary with seasonal shifts and environmental factors.

We generated a co-occurrence network using a novel similarity measure based on Fourier decomposition. This results in a co-occurrence network in which species cluster together, which occurred at similar times of the year. This approach differs from previous methods that rely directly on the raw time series signals (Ma et al., 2016; Lima-Mendez et al., 2015; Ma et al., 2020). By utilizing Fourier decomposition, we generated comprehensive temporal profiles for each ASV, providing a more nuanced understanding of co-occurrence dynamics. Consequently, the constructed network accurately reflects the temporal dynamics of each measured species' abundance, all in all revealing a clear seasonal cycle (see Fig. 2). The taxonomic composition of the communities defined by the partitioning of the co-occurrence network is a reflection of the prevailing food-web (Dunne et al., 2002): it starts in spring with photosynthetic primary producers

such as Bacillariophyta and continues through the summer (08TS, 09HS,10HS), while mixotrophs gain the upper hand in autumn (01TA,02TA, 03LW), leading to almost exclusively heterotrophic groups in winter dominated by the heterotrophic Syndiniales (04LW,05LW,07TS). It is notable that the spring clusters are taxonomically very diverse. This diversity can be explained by the rapid environmental changes during this period. Early spring clusters have high connections to winter clusters and are dominated by mixotrophic Dinophyceae, while late spring clusters (02TA) show more similarities to summer clusters (Stoecker et al., 2017). The ”late” spring cluster (08TS) reflects a bloom of primary producers with Ochrophyta (especially Bacillariophyta species), the dominant family (Obertegger et al., 2022). It is remarkable that Dinophyceae are present in almost all seasons, with the exception of the low light period, which is predominantly occupied by heterotrophic Syndiniales. This indicates that these mixotrophic organisms play a crucial role particularly in the intermediate phases of spring and autumn.

However, temporal co-occurrence does not imply interactions. To understand the causal influence between species we apply Convergent Cross-Mapping. Convergent Cross-Mapping results in a network with directed edges which indicate the strength of influence between ASVs. In general, most of the directed inter-cluster links are found between neighboring clusters. Our analysis revealed that by far not all species pairs, which are present at the same time, actually influence each other (see Fig. 3). A striking example is between clusters 06TS and 05LW, which were closely connected in the Co-occurrence network, while there are hardly any connections in the CCM network (see Fig. 3). This co-occurence without apparent causal connections could be explained by unique environmental conditions shaping both of these clusters, such as polar water supply. Even more pronounced is the separation of cluster 03LW, mainly heterotrophs, and 08TS, mainly phototrophs, which are tightly connected by co-occurrence but show not a single causal link in the CCM network . The organisms in these two clusters are primarily influenced by environmental parameters, particularly light. Additionally, these photosynthetic and heterotrophic organisms are sometimes preyed upon by the same predators (REF), such as Syndiniales. This explains the simultaneous occurrence and similar seasonality of these phytoplankton species but indicates that they do not have a direct influence on each other. The lack of mutual influence during the transition from dark to light periods is clearly visible in the CCM network (see Fig. 3). We interpret this gap between winter and spring clusters as a ’winter reset’. This phase is characterized by the predominance of parasites and Dinophycea. With the emergence of light, a new period of growth of primary producer communities begins, shaped by the prevailing environmental conditions. These conditions determine which species will succeed in the future. By reflecting causal interactions between species, the CCM network even stronger reflects the cyclic yearly food web structure than the co-occurrence network. The cycle begins with photoautotrophs (cluster 08TS) in early spring and ends with the hetero- and mixotrophs (cluster 01TA) in late autumn. As light intensity decreases, mixotrophs become more prevalent than photoautotrophs, leading to a shift towards a heterotrophic lifestyle and a transition from carbon fixation to consumption. This transition into a low light period is characterized by parasitic species, suggesting an ”eat and be eaten” scenario. The causal links from fall to winter are significantly less than between other seasons (except winter to spring). All of these causal links are related to Syndiniales, which can be explained by the parasitic lifestyle of Syndiniales, foraging upon mixotrophic species that are active during the transition autumn phase.

By analyzing species interactions across the annual cycle, we sought to identify communities that exhibit a stable structure under the prevailing environmental conditions. While the network analysis provides insights into species’ influences, it remains unclear how central and important each species is within the food web and how stable communities are in response to environmental fluctuations. To address these questions, we employed energy landscape analysis (ELA), a technique that allows quantifying the stability of communities in different environmental conditions. This approach helps identifying potential keystone species that play a pivotal role in maintaining community stability. It is generally assumed that ecological systems are governed by a limited number of ecological variables and drivers (Schröder et al., 2005). To identify these keystone species and the environemntal factors that are important to stabilize communities, we specifically analyzed the winter and summer communities. Interestingly, we found that winter communities are more stable under changing environmental conditions than summer communities Section 4 Figure S5 and S6. Stable summer communities consist of fewer species and are more vulnerable to changes in environmental conditions than stable winter communities (refer to the table of references).

We confirmed this observation by simulating a typical winter or summer day in the polar or Atlantic regions, and assessed the stability of the previously identified stable communities. The results indicate that a typical winter community has many stability values in both Arctic and Atlantic environmental

conditions. In contrast, a typical summer community is very sensitive to environmental conditions. This suggests that an Atlantic community will not maintain its structure when it experiences Arctic conditions. Our study indicates that Atlantic summer communities are vulnerable to polar influences. Within these communities, the Bacillariophyta appear particularly sensitive, whereas Chlorophyceae are more tolerant to polar conditions.

We used Co-Occurrence Networks (CON), Convergent Cross Mapping (CCM), and Energy Landscape Analysis (ELA) to analyze the complex dynamics of Arctic microbial communities. In traditional ecological theory, keystone species are often defined as those with the most biomass. However, this subjective evaluation does not necessarily indicate a central role in the ecosystem. Here, we use network analysis methods to define keystone species as those with the most significant role in the interaction network. This approach allows us to identify keystone species not only in summer but also in winter and other seasons. Our research has shown that indeed some of the keystone species show a high abundance for example Fragilariopsis or Chaetoceros. However, in addition to these common species, there are also other species that may not have been detected using more traditional methods.

While our approach focuses on the specific interactions within and between clusters, Ushio et al. provides a more general framework for predicting community diversity based on interaction capacity, temperature and abundance. The emphasis on mechanistic explanations for observed ecological patterns distinguishes the two approaches. Our methodology provides a comprehensive understanding of keystone species in a specific context, while Ushio's study provides broader insights into the factors influencing community diversity in different ecosystems. Both studies use similar techniques such as correlation and CCM (Ushio, 2022).

Fujita's study used controlled experiments with six isolated community replicates, subjected to diverse treatments over 110 days. Regarding Takens' Theorem and Convergence Cross Mapping, Fujita et al. used Simplex projection to forecast population size, while our study utilized pairwise Convergence Cross Mapping on ASV time series signals within clusters to predict potentially keystone species (Fujita et al., 2023).

The results presented in this study not only have practical implications for ecosystem management by improving our understanding and ability to predict change in complex ecological systems but also provide systematic and mechanistic insights into the mechanisms responsible for shaping and maintaining spatiotemporal heterogeneity in ecosystem composition (Suzuki et al., 2020).

CONFLICT OF INTEREST STATEMENT

The authors declare that the research was conducted in the absence of any commercial or financial relationships that could be construed as a potential conflict of interest.

AUTHOR CONTRIBUTION

WJvA, CB, MW and KM are responsible for the sampling design. WJvA contributed oceanographic data. EO devised the project, the main conceptual ideas and study outline. EO and RMK designed the model and the computational framework, analysed the data and wrote the initial draft. RMK carried out the implementation. EO, RMK and OP interpreted the data, conceptualized and drafted the manuscript. OE and OP advised data evaluation and data interpretation and revised and finalized the manuscript. All authors contributed to improving the final manuscript, by contributions to the scientific interpretation of the data and the discussion of results.

ACKNOWLEDGEMENTS

Computational infrastructure and support were provided by the Centre for Information and Media Technology at Heinrich Heine University Düsseldorf. Thanks to Kenta Suzuki for supporting us in adapting rELA to our needs. We thank Theresa Hargesheimer, Jana Bäger and Daniel Scholz for technical support of the RAS deployment. Moreover we thank the captains and crews of RV Polarstern for excellent support at sea, and the chief scientists for leading the various expeditions conducted for this study. Ship time for RV Polarstern was provided under grants AWI_PS99_00, AWI_PS100_01, AWI_PS107_05, AWI_PS114_01, AWI_PS121_01 of RV Polarstern. Our special thanks go to S. Neuhaus for bioinformatic support, K. Oetjen and S. Ziemann for excellent technical support in the laboratory, Martina Löbl for coordination of the FRAM-project.

FUNDING

This work was further supported by The Deutsche Forschungsgemeinschaft (DFG) under grant number EB 418/6-1 (From Dusk till Dawn) and under Germany's Excellence Strategy - EXC-2048/1 - project ID 390686111 (CEPLAS)(EO and OE).

SUPPLEMENTAL DATA

Supplementary Material - Methods

Supplementary Material - Networks

DATA AVAILABILITY STATEMENT

The python codes will be available at `https://github.com/rakro101/otter.git` after acceptance.

REFERENCES

Arrigo, K. R., Perovich, D. K., Pickart, R. S., Brown, Z. W., Van Dijken, G. L., Lowry, K. E., et al. (2012). Massive phytoplankton blooms under arctic sea ice. *Science* 336, 1408–1408

Arrigo, K. R., van Dijken, G. L., and Strong, A. L. (2015). Environmental controls of marine productivity hot spots around a ntarctica. *Journal of Geophysical Research: Oceans* 120, 5545–5565

Assmy, P., Fernández-Méndez, M., Duarte, P., Meyer, A., Randelhoff, A., Mundy, C. J., et al. (2017). Leads in arctic pack ice enable early phytoplankton blooms below snow-covered sea ice. *Scientific reports* 7, 40850

Barber, D. G., Hop, H., Mundy, C. J., Else, B., Dmitrenko, I. A., Tremblay, J.-E., et al. (2015). Selected physical, biological and biogeochemical implications of a rapidly changing arctic marginal ice zone. *Progress in Oceanography* 139, 122–150

Becker, O. M. and Karplus, M. (1997). The topology of multidimensional potential energy surfaces: Theory and application to peptide structure and kinetics. *The Journal of chemical physics* 106, 1495–1517

Blondel, V. D., Guillaume, J.-L., Lambiotte, R., and Lefebvre, E. (2008). Fast unfolding of communities in large networks. *Journal of statistical mechanics: theory and experiment* 2008, P10008

Bluhm, B. A., Gradinger, R., and Hopcroft, R. R. (2011). Arctic ocean diversity: synthesis. *Marine Biodiversity* 41, 1–4

Bluhm, B. A., Swadling, K. M., and Gradinger, R. (2017). Sea ice as a habitat for macrograzers. *Sea ice* , 394–414

Booth, B. C. and Horner, R. A. (1997). Microalgae on the arctic ocean section, 1994: species abundance and biomass. *Deep Sea Research Part II: Topical Studies in Oceanography* 44, 1607–1622

Cardinale, B. J., Duffy, J. E., Gonzalez, A., Hooper, D. U., Perrings, C., Venail, P., et al. (2012). Biodiversity loss and its impact on humanity. *Nature* 486, 59–67

Clement Kinney, J., Maslowski, W., Osinski, R., Jin, M., Frants, M., Jeffery, N., et al. (2020). Hidden production: On the importance of pelagic phytoplankton blooms beneath arctic sea ice. *Journal of Geophysical Research: Oceans* 125, e2020JC016211

Crawford, D. W., Cefarelli, A. O., Wrohan, I. A., Wyatt, S. N., and Varela, D. E. (2018). Spatial patterns in abundance, taxonomic composition and carbon biomass of nano-and microphytoplankton in subarctic and arctic seas. *Progress in Oceanography* 162, 132–159

Duffy, J. E. (2009). Why biodiversity is important to the functioning of real-world ecosystems. *Frontiers in Ecology and the Environment* 7, 437–444

Dunne, J. A., Williams, R. J., and Martinez, N. D. (2002). Network structure and biodiversity loss in food webs: robustness increases with connectance. *Ecology letters* 5, 558–567

Eppley, R. W. and Peterson, B. J. (1979). Particulate organic matter flux and planktonic new production in the deep ocean. *Nature* 282, 677–680

Fernández-Méndez, M., Katlein, C., Rabe, B., Nicolaus, M., Peeken, I., Bakker, K., et al. (2015). Photosynthetic production in the central arctic ocean during the record sea-ice minimum in 2012. *Biogeosciences* 12, 3525–3549

Fortier, M., Fortier, L., Michel, C., and Legendre, L. (2002). Climatic and biological forcing of the vertical flux of biogenic particles under seasonal arctic sea ice. *Marine Ecology Progress Series* 225, 1–16

Frey, K. (2017). Arctic ocean primary productivity. *In: Arctic Report Card 2017, NOAA, http://www. arctic. noaa. gov/Report-Card/Report-Card-2017/ArtMID/7798/ArticleID/701/Arctic-Ocean-Primary-Productivity*

Fujita, H., Ushio, M., Suzuki, K., Abe, M. S., Yamamichi, M., Iwayama, K., et al. (2023). Alternative stable states, nonlinear behavior, and predictability of microbiome dynamics. *Microbiome* 11, 63

Gosselin, M., Levasseur, M., Wheeler, P. A., Horner, R. A., and Booth, B. C. (1997). New measurements of phytoplankton and ice algal production in the arctic ocean. *Deep Sea Research Part II: Topical Studies in Oceanography* 44, 1623–1644

Guimera, R. and Nunes Amaral, L. A. (2005). Functional cartography of complex metabolic networks. *nature* 433, 895–900

Hardge, K., Peeken, I., Neuhaus, S., Lange, B. A., Stock, A., Stoeck, T., et al. (2017). The importance of sea ice for exchange of habitat-specific protist communities in the central arctic ocean. *Journal of Marine Systems* 165, 124–138

Hooper, D. U., Adair, E. C., Cardinale, B. J., Byrnes, J. E., Hungate, B. A., Matulich, K. L., et al. (2012). A global synthesis reveals biodiversity loss as a major driver of ecosystem change. *Nature* 486, 105–108

Ives, A. R. and Carpenter, S. R. (2007). Stability and diversity of ecosystems. *science* 317, 58–62

Javier, P. J. E. A., Liponhay, M. P., Dajac, C. V. G., and Monterola, C. P. (2022). Causal network inference in a dam system and its implications on feature selection for machine learning forecasting. *Physica A: Statistical Mechanics and its Applications* 604, 127893

Joyce, K. E., Laurienti, P. J., Burdette, J. H., and Hayasaka, S. (2010). A new measure of centrality for brain networks. *PloS one* 5, e12200

Kraft, A., Nöthig, E.-M., Bauerfeind, E., Wildish, D. J., Pohle, G. W., Bathmann, U. V., et al. (2013). First evidence of reproductive success in a southern invader indicates possible community shifts among arctic zooplankton. *Marine Ecology Progress Series* 493, 291–296

Laza-Martínez, A., Arluzea, J., Miguel, I., and Orive, E. (2012). Morphological and molecular characterization of teleaulax gracilis sp. nov. and t. minuta sp. nov.(cryptophyceae). *Phycologia* 51, 649–661

Leu, E., Søreide, J., Hessen, D., Falk-Petersen, S., and Berge, J. (2011). Consequences of changing sea-ice cover for primary and secondary producers in the european arctic shelf seas: timing, quantity, and quality. *Progress in Oceanography* 90, 18–32

Lewis, K., Van Dijken, G., and Arrigo, K. R. (2020). Changes in phytoplankton concentration now drive increased arctic ocean primary production. *Science* 369, 198–202

Lima-Mendez, G., Faust, K., Henry, N., Decelle, J., Colin, S., Carcillo, F., et al. (2015). Determinants of community structure in the global plankton interactome. *Science* 348, 1262073

Lin, I., Liu, W. T., Wu, C.-C., Wong, G. T., Hu, C., Chen, Z., et al. (2003). New evidence for enhanced ocean primary production triggered by tropical cyclone. *Geophysical Research Letters* 30

Lin, Y.-C., Chin, C.-P., Yang, J. W., Chiang, K.-P., Hsieh, C.-h., Gong, G.-C., et al. (2022). How communities of marine stramenopiles varied with environmental and biological variables in the subtropical northwestern pacific ocean. *Microbial ecology* , 1–13

Loreau, M. and De Mazancourt, C. (2013). Biodiversity and ecosystem stability: a synthesis of underlying mechanisms. *Ecology letters* 16, 106–115

Ma, B., Wang, H., Dsouza, M., Lou, J., He, Y., Dai, Z., et al. (2016). Geographic patterns of co-occurrence network topological features for soil microbiota at continental scale in eastern china. *The ISME journal* 10, 1891–1901

Ma, B., Wang, Y., Ye, S., Liu, S., Stirling, E., Gilbert, J. A., et al. (2020). Earth microbial co-occurrence network reveals interconnection pattern across microbiomes. *Microbiome* 8, 1–12

Mann, D. G., Crawford, R., Round, F., et al. (2017). Bacillariophyta. *Handbook of the Protists* 7, 205–266

May, R. M. (1977). Thresholds and breakpoints in ecosystems with a multiplicity of stable states. *Nature* 269, 471–477

Meredith, M., Sommerkorn, M., Cassota, S., Derksen, C., Ekaykin, A., Hollowed, A., et al. (2019). Polar regions. *Special report on ocean and cryosphere in a changing chapter Intergovernmental Panel on Climate Change (IPCC). In Chapter 3 Polar Issues*

Mori, A. S., Furukawa, T., and Sasaki, T. (2013). Response diversity determines the resilience of ecosystems to environmental change. *Biological reviews* 88, 349–364

Nöthig, E.-M., Ramondenc, S., Haas, A., Hehemann, L., Walter, A., Bracher, A., et al. (2020). Summertime chlorophyll a and particulate organic carbon standing stocks in surface waters of the fram strait and the arctic ocean (1991–2015). *Frontiers in Marine Science* 7, 350

Obertegger, U., Flaim, G., Corradini, S., Cerasino, L., and Zohary, T. (2022). Multi-annual comparisons of summer and under-ice phytoplankton communities of a mountain lake. *Hydrobiologia* 849, 4613–4635

Priest, T., von Appen, W.-J., Oldenburg, E., Popa, O., Torres-Valdés, S., Bienhold, C., et al. (2023). Atlantic water influx and sea-ice cover drive taxonomic and functional shifts in arctic marine bacterial communities. *The ISME Journal* 17, 1612–1625

Richter-Menge, J. A. and Farrell, S. L. (2013). Arctic sea ice conditions in spring 2009–2013 prior to melt. *Geophysical Research Letters* 40, 5888–5893

Sala, O. E., Stuart Chapin, F., Armesto, J. J., Berlow, E., Bloomfield, J., Dirzo, R., et al. (2000). Global biodiversity scenarios for the year 2100. *science* 287, 1770–1774

Scheffer, M., Carpenter, S., Foley, J. A., Folke, C., and Walker, B. (2001). Catastrophic shifts in ecosystems. *Nature* 413, 591–596

Scheffer, M. and Carpenter, S. R. (2003). Catastrophic regime shifts in ecosystems: linking theory to observation. *Trends in ecology & evolution* 18, 648–656

Schröder, A., Persson, L., and De Roos, A. M. (2005). Direct experimental evidence for alternative stable states: a review. *Oikos* 110, 3–19

Shannon, P., Markiel, A., Ozier, O., Baliga, N. S., Wang, J. T., Ramage, D., et al. (2003). Cytoscape: a software environment for integrated models of biomolecular interaction networks. *Genome research* 13, 2498–2504

Soltwedel, T., Bauerfeind, E., Bergmann, M., Budaeva, N., Hoste, E., Jaeckisch, N., et al. (2005). Hausgarten: multidisciplinary investigations at a deep-sea, long-term observatory in the arctic ocean. *Oceanography*

Spreen, G., Kaleschke, L., and Heygster, G. (2008). Sea ice remote sensing using amsr-e 89-ghz channels. *Journal of Geophysical Research: Oceans* 113

Stephens, C. R., Heau, J. G., González, C., Ibarra-Cerdeña, C. N., Sánchez-Cordero, V., and González-Salazar, C. (2009). Using biotic interaction networks for prediction in biodiversity and emerging diseases. *PLoS One* 4, e5725

Stoecker, D. K., Hansen, P. J., Caron, D. A., and Mitra, A. (2017). Mixotrophy in the marine plankton. *Annual Review of Marine Science* 9, 311–335

Strass, V. H. and Nöthig, E. M. (1996). Seasonal shifts in ice edge phytoplankton blooms in the barents sea related to the water column stability. *Polar Biology* 16, 409–422

Sugihara, G., May, R., Ye, H., Hsieh, C.-h., Deyle, E., Fogarty, M., et al. (2012). Detecting causality in complex ecosystems. *science* 338, 496–500

Suter, E. A., Pachiadaki, M., Taylor, G. T., and Edgcomb, V. P. (2022). Eukaryotic parasites are integral to a productive microbial food web in oxygen-depleted waters. *Frontiers in Microbiology* 12, 764605

Suzuki, K., Nagaoka, S., Fukuda, S., and Masuya, H. (2020). Energy landscape analysis of ecological communities elucidates the phase space of community assembly dynamics. *Ecological Monographs*

Suzuki, K., Nakaoka, S., Fukuda, S., and Masuya, H. (2021). Energy landscape analysis elucidates the multistability of ecological communities across environmental gradients. *Ecological Monographs* 91, e01469

Thaler, M. and Lovejoy, C. (2014). Environmental selection of marine stramenopile clades in the arctic ocean and coastal waters. *Polar biology* 37, 347–357

Tragin, M. and Vaulot, D. (2018). Green microalgae in marine coastal waters: The ocean sampling day (osd) dataset. *Scientific Reports* 8, 14020

Ushio, M. (2022). Interaction capacity as a potential driver of community diversity. *Proceedings of the Royal Society B* 289, 20212690

van Leeuwe, M. A., Fenton, M., Davey, E., Rintala, J.-M., Jones, E. M., Meredith, M. P., et al. (2022). On the phenology and seeding potential of sea-ice microalgal species. *Elem Sci Anth* 10, 00029

Veilleux, B. (1979). An analysis of the predatory interaction between paramecium and didinium. *The Journal of Animal Ecology* , 787–803

von Appen, W.-J. (2017). Report on mooring processing of ps99. 2/ps100/ps101 recoveries. *epic.awi.de*

von Appen, W.-J., Wekerle, C., Hehemann, L., Schourup-Kristensen, V., Konrad, C., and Iversen, M. H. (2018). Observations of a submesoscale cyclonic filament in the marginal ice zone. *Geophysical Research Letters* 45, 6141–6149

Von Quillfeldt, C. (2000). Common diatom species in arctic spring blooms: their distribution and abundance. *Botanica Marina*

Watanabe, T., Hirose, S., Wada, H., Imai, Y., Machida, T., Shirouzu, I., et al. (2014). Energy landscapes of resting-state brain networks. *Frontiers in neuroinformatics* 8, 12

Zhao, Q., Van den Brink, P. J., Xu, C., Wang, S., Clark, A. T., Karakoç, C., et al. (2023). Relationships of temperature and biodiversity with stability of natural aquatic food webs. *Nature Communications* 14, 3507